Crystal Structure, Spectroscopic and Magnetic Properties of Two Unusual Compounds: [Cu(terpy)(N_3)Cl] and [{$Cu_{0.75}Ni_{0.25}$(terpy)(N_3)$_2$}$_2$]·2H_2O (terpy = 2,2′:6′,2″-terpyridine)†

Roberto Cortés,[a] Luis Lezama,[a] José I. R. Larramendi,[a] Maite Insausti,[a] José V. Folgado,[c] Gotzon Madariaga[b] and Teófilo Rojo*,[a]

[a] *Departamento de Química Inorgánica, Universidad del País Vasco, Aptdo 644, 48080 Bilbao, Spain*

[b] *Departamento de Física de la Materia Condensada, Universidad del País Vasco, Aptdo 644, 48080 Bilbao, Spain*

[c] *UIBCM, Departament de Química Inorgánica, Universitat de Valencia, Dr. Moliner 50, 46100 Burjassot, Valencia, Spain*

The crystal structures of two unusual complexes [Cu(terpy)(N_3)Cl] **1** and [{$Cu_{0.75}Ni_{0.25}$(terpy)-(N_3)$_2$}$_2$]·2H_2O **2** (terpy = 2,2′:6′,2″-terpyridine) have been determined at room temperature: **1**, space group $P2_1/c$, a = 10.586(5), b = 8.572(1), c = 16.396(3) Å, β = 100.69(3)°, Z = 4, $R = R'$ = 0.036, for 2818 reflections with $I \geqslant 3\sigma(I)$; **2**, space group $P2_1/c$, a = 10.195(5), b = 9.996(3), c = 15.866(8) Å, β = 91.10(5)°, Z = 4, $R = R'$ = 0.055 for 3134 reflections with $I \geqslant 3\sigma(I)$. Complex **1** possesses the first known co-ordination polyhedron including both halide (Cl) and pseudohalide (N_3) ligands. It shows a square-pyramidal topology for the copper(II), with the three nitrogen atoms of the terpy ligand and one terminal nitrogen atom of the azide group in the basal positions while the chloride atom is in the apical one. Compound **2** contains 25% of [{Ni(terpy)(N_3)$_2$}$_2$]·2H_2O and 75% of [{Cu-(terpy)(N_3)$_2$}$_2$]·2H_2O enclosed in the global lattice. It possesses (end-on) azide bridges and terminal azide ligands. The co-ordination polyhedron of the metal ion is a slightly distorted octahedron with the nitrogen atoms of the terpy ligand and a nitrogen atom of one of the azide bridging groups in the equatorial positions, while the nitrogen atoms of both the bridge and terminal azide groups occupy the axial positions. The pure copper phase related to compound **2** exhibits a discrete molecular topology; however, the pure nickel phase shows the same dimeric structure, which is useful for comparison. The magnetic properties of compound **2** can be explained by contributions from the isolated Cu_2 and Ni_2 entities, giving rise to global ferromagnetic interactions characterised by the parameters J = 20.1 cm^{-1}, D = −12.5 cm^{-1}, g_{Ni} = 2.26 and ρ = 0.76 corresponding to the copper proportion. The EPR measurements for both compounds reveal rhombic symmetries for the g tensors. Single-crystal EPR measurements on **2** show the presence of two magnetically different copper entities, with an antiferrodistortive ordering, in the lattice.

In past years our work has focused on the spectroscopic and magnetic properties of polynuclear copper(II) and nickel(II) compounds having tridentate aromatic amine ligands and pseudohalide ions.[1–5] It has been established that these tridentate amines favour a *cis* co-ordination of the bridging ligands around the nickel(II) or copper(II) ions. On the other hand, pseudohalides, especially azide ones, have been chosen to co-ordinate metals because of their ability to act as bridging entities in either a 'end-on' or 'end-to-end' fashion.[6–8] This bridging mode of the azide ligand is known to give antiferromagnetic interactions,[9] while the former type gives rise to ferromagnetic interactions, which are more scarce.[10]

One of the most useful synthetic strategies to obtain these pseudohalide compounds is where the initial product is the related halide complex. These complexes rapidly undergo substitution of their halide ligands by pseudohalide ones. As far as we are aware, there are no structurally characterised mixed halide–pseudohalide co-ordination compounds. Recently we have described a synthetic route to nickel(II) pseudohalide complexes having ferromagnetic interactions.[4]

Doped or substituted compounds are very common in co-ordination chemistry. However, it is very difficult to obtain solid solutions because it is very unusual for the two end members of the range to be isostructural. This presents a challenge because the products have interesting spectroscopic and magnetic properties.

In this paper we describe two unusual products obtained in a chemical synthesis the aim of which was to produce a copper–nickel bimetallic system. One of them represents, as far as we know, the first co-ordination compound with both halide and pseudohalide ligands, while the second constitutes the substitution of a nickel compound into a copper one, stabilising a dinuclear structure which does not exist for copper. Both have been structurally and spectroscopically characterised. The magnetic properties of the polynuclear compound are also discussed.

Experimental

Reagents.—All chemicals used in this work were reagent grade, used as commercially obtained.

Preparation of the Complexes [Cu(terpy)(N_3)Cl] **1** *and* [$Cu_{0.75}Ni_{0.25}$(terpy)(N_3)$_2$]·H_2O **2**.—Copper(II) chloride dihydrate (170 mg, 1 mmol) and terpy (2,2′:6′,2″-terpyridine) (233 mg, 1 mmol) were dissolved in methanol–water (*ca.* 1:1, 10 cm^3). This solution was added to a water–methanol solution

† *Supplementary data available:* see Instructions for Authors, *J. Chem. Soc., Dalton Trans.*, 1994, Issue 1, pp. xxiii–xxviii.

(30 cm^3) of the previously prepared compound [Ni(terpy)$(N_3)_2$]·H_2O (400 mg, 1 mmol).[2] The colour immediately changed from light to dark green. The solution was then left to stand at room temperature. Dark green large blocks of compound **2** appear in 3 d, which were filtered off and dried over P_2O_5 during 2 h. The filtered solution was left to stand again at room temperature for 1 week and different clearer green needle-prism crystals appeared. They were filtered off and corresponded to compound **1** [Found (Calc.) for **1**: C, 47.9 (48.1); H, 3.2 (3.0); Cu, 16.8 (17.0); N, 22.2 (22.4). Found (Calc.) for **2**: C, 44.7 (45.2); H, 3.1 (3.3); M, 15.6 (15.9); N, 31.8 (31.6%)]. Several atomic absorption analyses of large crystals of compound **2**, made on a Perkin-Elmer 300 AA atomic absorption/flame emission spectrophotometer, gave ≈75% Cu and ≈25% Ni.

Complex **1** has been also synthesized by reaction, in 1:1 proportion, of [Cu(terpy)Cl_2]·H_2O [11] with [Cu(terpy)$(N_3)_2$] [12] as a slow donor of azide ions.

Physical Measurements.—Infrared spectra were recorded for KBr discs, in the 4000–250 cm^{-1} region, with a Perkin-Elmer spectrophotometer. Magnetic susceptibilities were measured by the use of a SQUID SHE magnetometer in the temperature range 4.2–250 K. Experimental susceptibilities were corrected for both the diamagnetic contributions and the temperature-independent paramagnetism of the copper(II) and nickel(II) ions, estimated to be 60×10^{-6} and 100×10^{-6} cm^3 mol^{-1} per metal ion, respectively. Diamagnetic corrections were made with Pascal's constants. Q-Band EPR spectra of powdered samples were recorded at room temperature on a Bruker ESP 300 spectrometer equipped with a standard low-temperature device, calibrated by the NMR probe for the magnetic field, and a Hewlett-Packard 5342 A frequency counter for the microwave frequency. Single-crystal EPR spectra of complex **2** were recorded at room temperature on a Varian E15 spectrometer working at 35 GHz and using diphenylpicrylhydrazyl (dpph) ($g = 2.0037$) as internal reference. A single crystal was orientated by precession photographs and showed well developed ($\pm 1,0,0$) and ($0,0,\pm 1$) faces (see Fig. 1 for the crystal morphology and the crystallographic axes).

X-Ray Diffraction Data Collection, Structure Solution, and Refinement.—Preliminary cell dimensions for compounds **1** and **2** were calculated from precession photographs. A needle prism of **1** and a prismatic crystal of **2** were selected and mounted on an Enraf–Nonius CAD-4 diffractometer. Unit-cell parameters were determined from 25 reflections ($5.5 \leqslant \theta \leqslant 19.5°$) and refined by the least-squares method. Intensities were collected with graphite-monochromatized Mo-Kα radiation (λ 0.710 69 Å), using the ω–2θ scan technique. The most important features of the crystallographic data are summarised in Table 1. 7333 Reflections for the compound **1** and 8082 reflections for **2** were measured in the range $1.5 \leqslant \theta \leqslant 35°$, 2818 and 3134 of which were assumed as observed applying the condition $I \geqslant 3\sigma(I)$. Three reflections were measured every 2 h for each compound as intensity control, but significant intensity decay was not observed. The crystal orientation was monitored with three additional reflections checked every 200. Lorentz polarisation but no absorption corrections were made. The structures were solved with the SIR 88 [13] system of programs and refined by full-matrix least squares, using the X-RAY 72 system.[14] Scattering factors were taken from ref. 15.

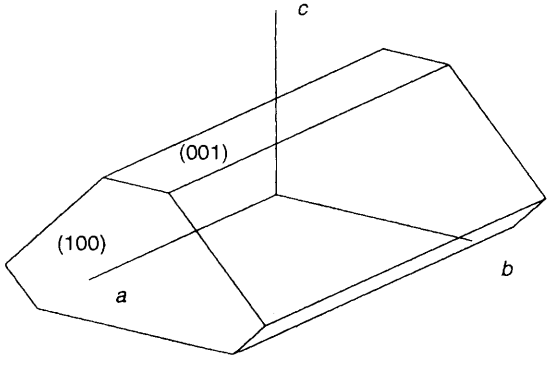

Fig. 1 Morphology of the crystal selected for the EPR measurements, showing the crystallographic axes

The structure of complex **1** was successfully refined in the space group $P2_1/c$. All non-hydrogen atoms were refined anisotropically. Hydrogen atoms of the terpyridine ligand were located from Fourier-difference syntheses and refined with a fixed isotropic thermal parameter, $U = 0.08$ Å^2. The final R factor was 0.036 ($R' = 0.036$). Maximum and minimum peaks in the final difference synthesis were 0.86 and −2.19 e Å^{-3}, respectively. Fractional atomic coordinates are listed in Table 2.

In the case of the compound **2** the structure was also refined in

Table 1 Data collection and structure refinement[a] for [Cu(terpy)(N_3)Cl] **1** and [$Cu_{0.75}Ni_{0.25}$(terpy)$(N_3)_2$]·H_2O **2**

Formula	$C_{15}H_{11}ClCuN_6$	$C_{15}H_{13}CuN_9O$
M	374.29	398.87
Crystal dimensions/mm	0.42 × 0.16 × 0.13	0.26 × 0.21 × 0.30
a/Å	10.586(5)	10.195(5)
b/Å	8.572(1)	9.996(3)
c/Å	16.396(3)	15.866(8)
β/°	100.69(3)	91.10(5)
U/Å^3	1462(1)	1617(2)
D_m/g cm^{-3}	1.70(2)	1.62(2)
D_c/g cm^{-3}	1.700	1.638
μ(Mo-Kα)/cm^{-1}	17.4	14.3
F(000)	756	812
Check reflections	2–34, 124, 122	1–34, 0.5–1, 3–13
No. measured reflections	7333	8082
No. independent reflections	6404	7092
h, k, l interval	17, 13, ±26	16, 16, ±25
No. variables, N_v	242	274
No. unique reflections, N_o	2818	3134
R[b]	0.036	0.055
R'[c]	0.036	0.055
Weighting parameter, p	0.000 98	0.001 24
S[d]	1.9	3.8

[a] Details in common: monoclinic, space group $P2_1/c$; $Z = 4$. [b] $(\Sigma||F_o| - |F_c||)/\Sigma|F_o|$. [c] $[\Sigma w(|F_o| - |F_c|)^2/\Sigma w|F_o|^2]^{\frac{1}{2}}$. [d] $[\Sigma w(|F_o| - |F_c|)^2/(N_o - N_v)]^{\frac{1}{2}}$.

Table 2 Fractional atomic coordinates (× 10^4, × 10^5 for Cu and Cl) for [Cu(terpy)(N_3)Cl]

Atom	x	y	z
Cu	70 070(3)	7 732(3)	8 485(2)
Cl	84 786(5)	29 897(7)	12 316(3)
N(1)	8 386(2)	−958(2)	1 033(1)
C(11)	8 905(2)	−1 667(3)	1 740(1)
C(12)	9 802(3)	−2 849(3)	1 784(1)
C(13)	185(2)	−3 318(3)	1 067(2)
C(14)	9 685(2)	−2 571(3)	328(1)
C(15)	8 787(2)	−1 407(2)	331(1)
N(2)	7 257(2)	428(2)	−292(1)
C(21)	8 170(2)	−564(2)	−424(1)
C(22)	8 455(2)	−748(3)	−1 214(1)
C(23)	7 768(3)	148(3)	−1 848(1)
C(24)	6 810(2)	1 137(3)	−1 709(1)
C(25)	6 562(2)	1 252(2)	−910(1)
N(3)	5 506(2)	2 038(2)	184(1)
C(31)	5 542(2)	2 180(2)	−640(1)
C(32)	4 682(2)	3 122(3)	−1 154(2)
C(33)	3 753(2)	3 912(3)	−824(2)
C(34)	3 705(2)	3 753(3)	7(2)
C(35)	4 601(2)	2 800(3)	492(2)
N(4)	6 208(2)	625(3)	1 835(1)
N(5)	6 550(2)	7(3)	2 424(1)
N(6)	6 851(3)	−639(4)	3 062(2)

the $P2_1/c$ space group. All the metal atoms were considered as copper [nickel(II) and the copper(II) ions are hardly distinguishable by X-ray diffraction and the proportion of each cannot be obtained in the refinement process]. The non-hydrogen atoms were refined anisotropically and the hydrogens located from Fourier-difference syntheses and assigned isotropical thermal parameters. The final R was 0.055 (R' = 0.055) for all observed reflections. Maximum and minimum peaks in the final difference synthesis were 1.2 and −2.4 e Å^{-3}, respectively. Final atomic parameters are listed in Table 3.

Additional material available from the Cambridge Crystallographic Data Centre comprises H-atom coordinates, thermal parameters and remaining bond lengths and angles.

Results and Discussion

Crystal Structure of Complex **1**.—This structure consists of discrete molecules [Cu(terpy)(N_3)Cl] in which the copper atom is bonded to the three nitrogen atoms of the terpy ligand [Cu–N(1), –N(2), –N(3) 2.064(7), 1.959(8), 2.06(2) Å] and unusually co-ordinated to both halide [Cu–Cl 2.46(1) Å] and pseudohalide ions [Cu–N(4) 1.96(2) Å]. An ORTEP[16] diagram of the asymmetric unit is shown in Fig. 2, while Table 4 compiles selected bond distances and angles. The geometry of the copper(II) co-ordination polyhedron is a distorted square pyramid, where the four nitrogen atoms occupy the basal positions and the chlorine atom the apical one. This co-ordination may be considered as 4 + 1, which is usually found for five-co-ordinate copper(II) complexes.[17] The four nitrogen atoms are practically coplanar, the copper(II) ion being out of this plane by 0.25 Å. As far as we are aware this is the first complex with both halide and pseudohalide ligands.

This kind of distorted square-pyramidal co-ordination (4 + 1) is also observed in the related dichloride[18] and diazide[12] complexes, having apical distances of Cu–Cl 2.469(2) and Cu–N 2.21(2) Å, respectively. The corresponding basal distances are 2.252(2) (dichloride) and 1.96 Å (diazide).

The azide ligand is practically linear [N(4)–N(5)–N(6) 176.4(3)°]. The distortion of the copper co-ordination polyhedron from square pyramidal to trigonal bipyramidal has been calculated by quantification of the Muetterties and Guggenberger description.[19] The value obtained (Δ = 0.76) indicates a topology close to a regular elongated square pyramid.

Crystal Structure of Complex **2**.—The structure consists of [M(terpy)(N_3)$_2$]·H_2O (M = Cu or Ni) units linked together to give dinuclear [{M(terpy)(N_3)$_2$}$_2$]·2H_2O. The dinuclear unit is bridged by two (end-on) azide groups and has a M···M distance of 3.59(1) Å. These dimers have molecular C_i symmetry, which is also the crystallographic one. Although in general centrosymmetry inhibits heterodinuclearity, in this case X-rays cannot distinguish copper from nickel and heterodinuclearity cannot be discarded. Taking into account the proportions of copper and nickel obtained from the atomic absorption analysis, two possibilities may be then considered and further analysed: (*a*) the existence of Cu–Ni complexes together with Cu_2 ones in 1:1 proportion; (*b*) the existence of

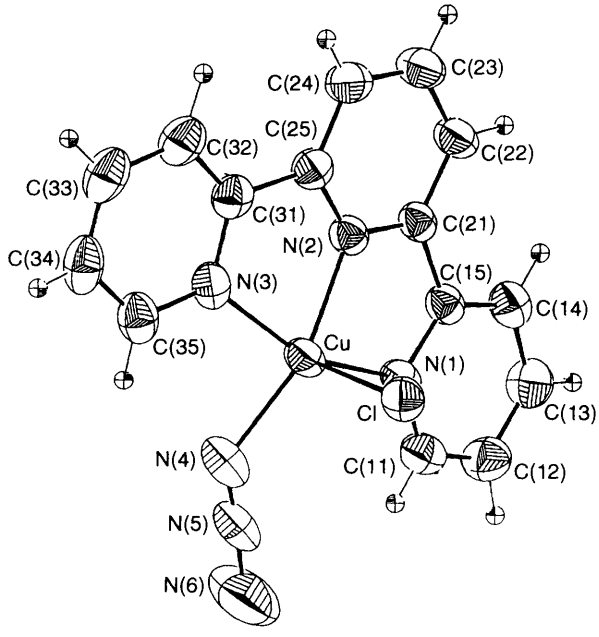

Fig. 2 An ORTEP drawing of the [Cu(terpy)(N_3)Cl] complex together with the atom numbering. Thermal ellipsoids of non-hydrogen atoms are plotted at the 70% probability level. Hydrogen atoms are given an arbitrary radius

Table 3 Fractional atomic coordinates (×10^4, ×10^5 for Cu) for [$Cu_{0.75}Ni_{0.25}$(terpy)(N_3)$_2$]·H_2O

Atom	x	y	z
Cu	85 221(4)	9 642(4)	48 673(2)
N(1)	7 343(3)	646(3)	5 798(2)
C(11)	7 458(3)	1 394(3)	6 489(2)
C(12)	6 640(4)	1 196(4)	7 170(2)
C(13)	5 708(4)	180(4)	7 098(2)
C(14)	5 616(4)	−617(4)	6 390(2)
C(15)	6 490(3)	−367(3)	5 742(2)
N(2)	7 507(3)	−668(3)	4 417(2)
C(21)	6 572(3)	−1 115(3)	4 935(2)
C(22)	5 784(4)	−2 196(4)	4 736(2)
C(23)	5 952(5)	−2 802(4)	3 961(3)
C(24)	6 884(4)	−2 332(4)	3 423(2)
C(25)	7 639(4)	−125 4(4)	3 672(2)
N(3)	9 144(3)	2 404(3)	5 702(2)
C(31)	10 065(4)	3 346(4)	5 568(2)
C(32)	10 378(4)	4 307(4)	6 180(3)
C(33)	9 726(4)	4 296(4)	6 924(2)
C(34)	8 766(4)	3 347(4)	7 062(2)
C(35)	8 493(3)	2 431(3)	6 430(2)
N(4)	10 000(3)	803(3)	4 089(2)
N(5)	10 628(3)	1 670(3)	3 794(2)
N(6)	11 263(4)	2 457(4)	3 479(2)
O(w)	6 361(4)	5 685(5)	6 382(3)
N(7)	7 110(3)	3 346(4)	4 422(2)
N(8)	7 344(4)	2 460(4)	4 096(2)
N(9)	6 818(5)	4 368(4)	4 795(3)

Table 4 Selected bond distances (Å) and angles (°) for [Cu(terpy)(N_3)Cl]

Copper co-ordination sphere			
Cu–N(1)	2.064(7)	Cu–N(2)	1.959(8)
Cu–N(3)	2.06(2)	Cu–N(4)	1.96(2)
Cu–Cl	2.46(1)	Cu···Cu^I	4.81(7)
N(1)–Cu–N(2)	79.28(7)	N(1)–Cu–N(3)	155.61(7)
N(1)–Cu–N(4)	103.52(8)	N(1)–Cu–Cl	96.93(6)
N(2)–Cu–N(3)	78.59(7)	N(2)–Cu–N(4)	158.70(8)
N(2)–Cu–Cl	99.73(5)	N(3)–Cu–N(4)	93.57(9)
N(3)–Cu–Cl	96.78(6)	N(4)–Cu–Cl	100.85(7)
Average values in terpy ligand			
C–N	1.34(3)	C–C	1.43(5)
C–H	0.9(1)		
C–C–C	122(3)	C–C–N	117(5)
C–N–C	119(3)		
Azide ligand			
N(4)–N(5)	1.10(1)	N(5)–N(6)	1175(9)
Cu–N(4)–N(5)	129.1(2)	N(4)–N(5)–N(6)	176.4(3)

Symmetry relation: I 1 − x, −y, −z.

75% copper dimers and 25% nickel ones. A perspective view of the molecule is given in Fig. 3, together with the atom-numbering system. The significant bond distances and angles are given in Table 5 together with those of the corresponding pure nickel phase for comparison. Each metal atom displays distorted octahedral co-ordination, being linked to the three nitrogen atoms of the terpy ligand [M–N(1), –N(2), –N(3) 1.95(3), 2.05(1), 2.05(1) Å] and three nitrogen atoms of the azide ligands [M–N(4), –N(4^{I}), –N(8) 1.97(3), 2.83(3), 2.26(2) Å] (I = 2 − x, −y, 1 − z) in *cis-trans* position. The co-ordination may be considered as 4 + 1 + 1, as usually found for Jahn–Teller-active six-co-ordinate copper(II) complexes.[17] The pure nickel(II) compound[2] contains similar molecular entities but the absence of the Jahn–Teller effect leads, obviously, to a more regular co-ordination polyhedron. Although the structure of the pure copper(II) compound is monomeric,[12] related copper compounds with this type of bridging show Cu–N(4^{I}) distances ranging from 2.85 to 3.37 Å.[1,5] Thus, we cannot know what Cu–N(4^{I}) distance the pure copper(II) dimer would have. Notwithstanding, considering the Ni–N(4^{I}) distance of 2.2 Å in the pure nickel dimer, 25% of this in the Cu–Ni compound [M–N(4^{I}) 2.83 Å] would require a Cu–N(4^{I}) distance of 3.06 Å. This distance is in the range observed for related copper(II) dimers. The atoms M, N(1), N(4), N(8), M^{I}, N(1^{I}), N(4^{I}), N(8^{I}) are in a plane [largest deviations 0.007(8) Å]. The azide ligand is bonded in asymmetrical fashion [M–N(4^{I}) 0.86 Å longer than M–N(4)], which is the most significant difference with respect to the pure nickel(II) compound which shows higher symmetry [Ni–N(4^{I}) 0.16 Å longer than Ni–N(4)]. This large axial distance is typical of the semico-ordination effect of the copper(II) ion and would be less for Ni^{II} and thus unfavourable for the existence of mixed Cu–Ni complexes; however, this is not conclusive. For compound **2** both the bridging and terminal azide groups are quasi-linear, with N–N–N angles of 176.2(4) and 179.0(5)°, respectively.

The small N(terpy)–M–N(terpy) bond angles [average 79.4(1)°] and N(4)–M–N(4^{I}) [84.9(1)°] results in deviations of remaining bond angles involving the metal as central atom from the regular octahedral value. The distortion from an octahedron to a trigonal prism (Δ) for this complex has been examined using the Muetterties and Guggenberger description,[19] giving a value

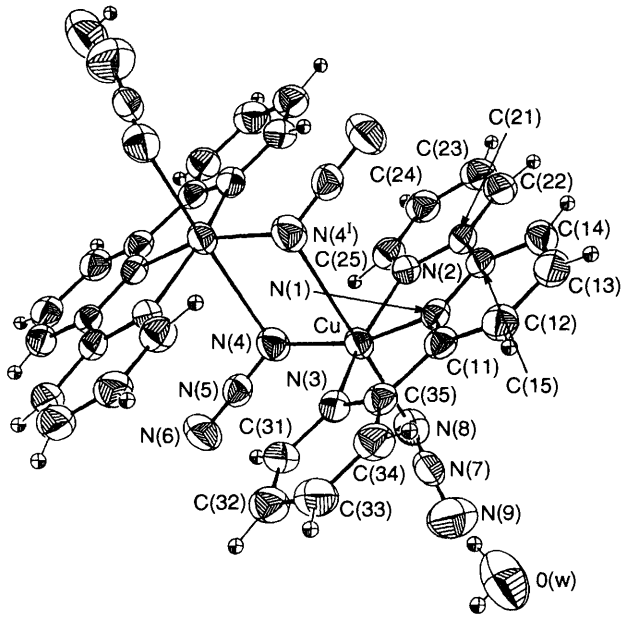

Fig. 3 Perspective view of [{$Cu_{0.75}Ni_{0.25}$(terpy)$(N_3)_2$}$_2$]·2H_2O. Thermal ellipsoids of non-hydrogen atoms are plotted at the 70% probability level. Hydrogen atoms are given an arbitrary radius

Table 5 Selected bond distances (Å) and angles (°) for [{$Cu_{0.75}Ni_{0.25}$(terpy)$(N_3)_2$}$_2$]·2H_2O compared with those for [{Ni(terpy)$(N_3)_2$}$_2$]·2H_2O

	Cu–Ni	Ni		Cu–Ni	Ni
Metal co-ordination sphere*					
M–N(1)[N(2)]	1.95(3)	1.966(8)	M–N(2)[N(1)]	2.05(1)	2.081(8)
M–N(3)	2.05(1)	2.101(8)	M–N(4)	1.97(3)	2.038(8)
M–N(4^{I})	2.83(3)	2.198(8)	M–N(8)[N(5)]	2.26(2)	2.071(9)
M ··· M^{I}	3.59(1)	3.276(1)	M ··· M^{II}	7.45(1)	7.423(2)
N(1)[N(2)]–M–N(2)[N(1)]	79.6(1)	77.6(3)	N(1)[N(2)]–M–N(3)	79.2(1)	78.8(3)
N(1)[N(2)]–M–N(4)	162.0(1)	166.3(3)	N(1)[N(2)]–M–N(8)[N(5)]	100.9(1)	98.4(3)
N(1)[N(2)]–M–N(4^{I})	77.5(1)	87.7(3)	N(2)[N(1)]–M–N(3)	158.6(1)	156.2(3)
N(2)[N(1)]–M–N(4)	95.9(1)	100.3(3)	N(2)[N(1)]–M–N(8)[N(5)]	94.5(1)	89.5(3)
N(2)[N(1)]–M–N(4^{I})	88.1(1)	90.5(3)	N(3)–M–N(4)	103.4(1)	103.3(3)
N(3)–M–N(8)[N(5)]	92.3(1)	91.2(3)	N(3)–M–N(4^{I})	84.6(1)	91.3(3)
N(4)–M–N(4^{I})	84.9(1)	78.7(3)	M–N(4)–M^{I}	95.1(1)	101.3(3)
Average values in the terpy ligand					
C–N	1.34(5)	1.34(2)	C–C	1.43(4)	1.42(3)
C–H	0.9(1)	0.9(1)			
C–C–C	122(3)	123(3)	C–C–N	117(5)	118(2)
C–N–C	120(2)	119(2)			
Azide ligands					
N(4)–N(5)	1.180(1)		N(5)–N(6)	1.14(1)	
N(8)–N(7)	1.055(6)		N(7)–N(9)	1.220(7)	
N(4)–N(41)		1.181(9)	N(41)–N(42)		1.154(10)
N(5)–N(51)		1.20(1)	N(51)–N(52)		1.16(2)
M–N(4)–N(5)	128.0(5)		N(4)–N(5)–N(6)	176.2(4)	
M–N(8)–N(7)	114.4(8)		N(8)–N(7)–N(9)	179.0(5)	
M–N(4)–N(41)		126.0(7)	N(4)–N(41)–N(42)		175.8(11)
M–N(5)–N(51)		132.4(5)	N(5)–N(51)–N(52)		176.8(11)

Symmetry relations: I 2 − x, −y, 1 − z; II 1 − x, −y, 1 − z.

* The atoms indicated in square brackets correspond to those in the pure nickel compound.

equal to 0.03 which clearly indicates that the polyhedron approximates octahedral geometry. The water molecule acts as a buffer between the dimeric units through hydrogen bonds [O(w)–H(1)···N(6^{II}) and O(w)–H(2)···N(9)], the d_{ON} lengths being 3.06(1) and 2.89(1) Å, respectively (symmetry code II $1-x, -y, 1-z$). A similar behaviour is exhibited by the pure nickel phase.

In both complexes **1** and **2** the terpy ligand may be considered as rigid and quasi-planar. The average C–C and C–N bond distances in the pyridine rings of this ligand are 1.43(5), 1.34(3), and 1.43(4), 1.34(3) Å for **1** and **2**, respectively. The bond distances and angles in terpy are in good agreement with those in the literature.[20]

Infrared Spectroscopy.—The major interest in the IR spectra of the studied compounds is centred in the bands of the azide groups. When this pseudohalide co-ordinates to a transition metal an intense band can be observed in the 2075–2000 cm^{-1} region, which corresponds to the azide antisymmetric stretch [$\nu_{asym}(N_3)$] and is used to predict the co-ordination mode.

Complex **1** shows one intense absorption band at 2015 cm^{-1}, which must be assigned to the antisymmetric stretch of the terminal azide group present in the crystal structure. However, **2** exhibits two intense bands, corresponding to the $\nu_{asym}(N_3)$ vibration, at 2060 and 2020 cm^{-1}. These bands must be assigned to the bridging and terminal azide groups respectively, in good accord with the crystallographic results.

For compound **1** the azide symmetric stretch, $\nu_{sym}(N_3)$, appears as a weak band at about 1300 cm^{-1}, in good accord with its crystal structure showing a terminal azide ligand. In the case of **2** the $\nu_{sym}(N_3)$ vibration can be observed as a medium band, at 1300 cm^{-1}, in agreement with its crystal structure containing both end-on azido bridges and terminal azide ligands.[21] A band at 610 cm^{-1} is observed for **1**, which corresponds to the $\delta(N_3)$ vibration mode. For **2** two bands, corresponding to the bending vibration, appear at 600 and 615 cm^{-1}, in accord with the existence of azide bridging groups.

EPR Spectroscopy.—The polycrystalline powder Q-band EPR spectra of compounds **1** and **2**, at 4.2 K, are shown in Fig. 4. That of **1** exhibits a rhombic symmetry for the g tensor, with $g_1 = 2.185$, $g_2 = 2.132$ and $g_3 = 2.058$. These values do not reflect the approximate square-pyramidal geometry of the CuN_4Cl entity in this compound, because two g values ($g_{\|}$ and $g_{\perp}$) are expected for a $d_{x^2-y^2}$ ground state in a C_{4v} symmetry. Exchange interactions between differently oriented polyhedra having the canting angle 2γ [18] would induce a coupled g tensor with g_1^{ex}, g_2^{ex}, g_3^{ex}. The canting angle can be calculated from equation (1) [18] and the value obtained, 74.7°, is in reasonable

$$\cos 2\gamma = \frac{g_1^{ex} - g_2^{ex}}{g_1^{ex} + g_2^{ex} - 2g_3^{ex}} \quad (1)$$

agreement with the crystallographic value $2\gamma'$ (79.1°).[18] Because the $g_{\perp}$ components of an axial molecular g tensor are presumably located in the best equatorial plane, 2γ is defined as the canting angle between the normals to the equatorial planes of the two interacting polyhedra, and is not necessarily equal to $2\gamma'$ (crystallographic canting angle between the long axes of the two interacting square pyramids). This result is very similar to that found for the related dichloro [18] and diazido [12] complexes. The resulting molecular g tensors, calculated by the expression given in ref. 18, are $g_{\|} = 2.25$, $g_{\perp} = 2.06$, in good agreement with a $d_{x^2-y^2}$ ground state. For complex **2** the Q-band spectrum is typical of a monomeric copper(II) ion with an axial environment, leading to $g_{\|} = 2.252$ and $g_{\perp} = 2.051$. However, the X-band spectrum shows, in addition to this large $g = 2$ signal, a very weak signal at 'half-field' position which is indicative of the existence of a triplet state. This situation is similar to that found for related copper(II) dimers having very weak magnetic interactions.[1]

The absence of signals due to a coupled Cu–Ni system (signals due to Kramer doublets should appear) would be in accord with the existence of isolated Cu–Cu and Ni–Ni dimers. The EPR bands exhibited would correspond to the copper(II) dimers, the nickel system not being observed.

A single-crystal EPR study was carried out for compound **2**. The crystallographic axes were determined by means of precession photographs. It can be considered that since the monoclinic angle β is 91.1° the crystal has been rotated (within the experimental laboratory error) around three orthogonal axes parallel to the crystallographic ones. Two signals of equal intensity were observed upon rotation in the *ab* and *bc* planes whereas only one was found in the *ac* plane (Fig. 5). A complete analysis of the angular dependence of the g factors provided the principal values and orientations reported in Table 6. They are compatible with the presence of two magnetically non-equivalent sites for the copper(II) ions, but with the same geometry, and with their preferred axes mutually perpendicular (*i.e.* with an antiferrodistortive ordering in the lattice).

Table 6 Principal values and orientations of the g tensors compared to those for the molecular x, y, z directions (see text)

	Signal 1				Signal 2		
	a	*b*	*c*		*a*	*b*	*c*
$g_1 = 2.250$	51	50	116	$g_1 = 2.253$	51	49	115
$g_2 = 2.063$	113	42	58	$g_2 = 2.065$	113	43	57
$g_3 = 2.054$	48	100	44	$g_3 = 2.054$	48	100	44
g_z	59	50	124	g_z	58	50	122
g_y	114	40	60	g_x	114	41	60
g_x	44	88	46	g_y	44	89	46

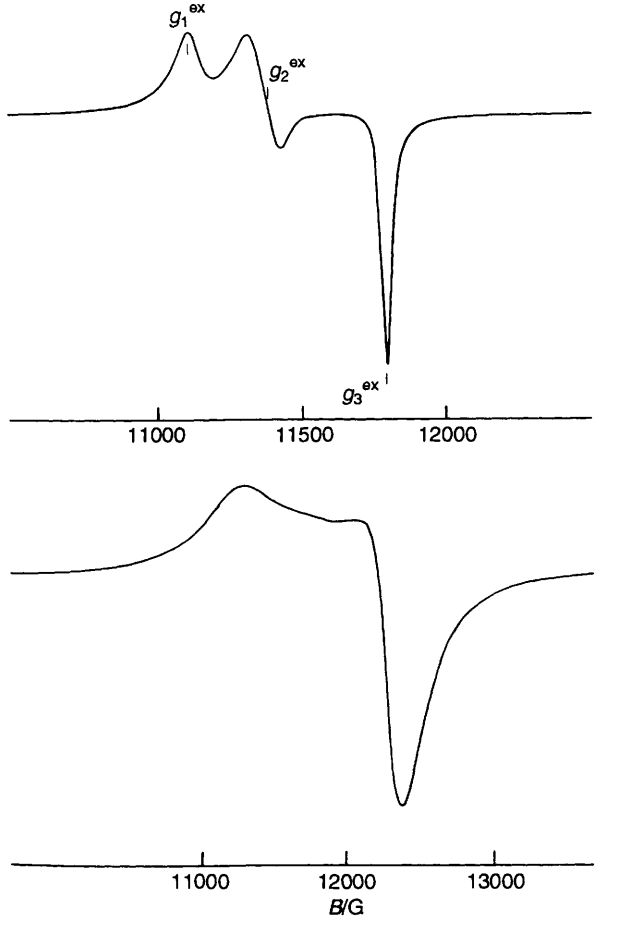

Fig. 4 Q-Band EPR powder spectra, at 4.2 K, of (*a*) [Cu(terpy)(N_3)Cl] and (*b*) [{$Cu_{0.75}Ni_{0.25}$(terpy)(N_3)$_2$}$_2$]·$2H_2O$. G = 10^{-4} T

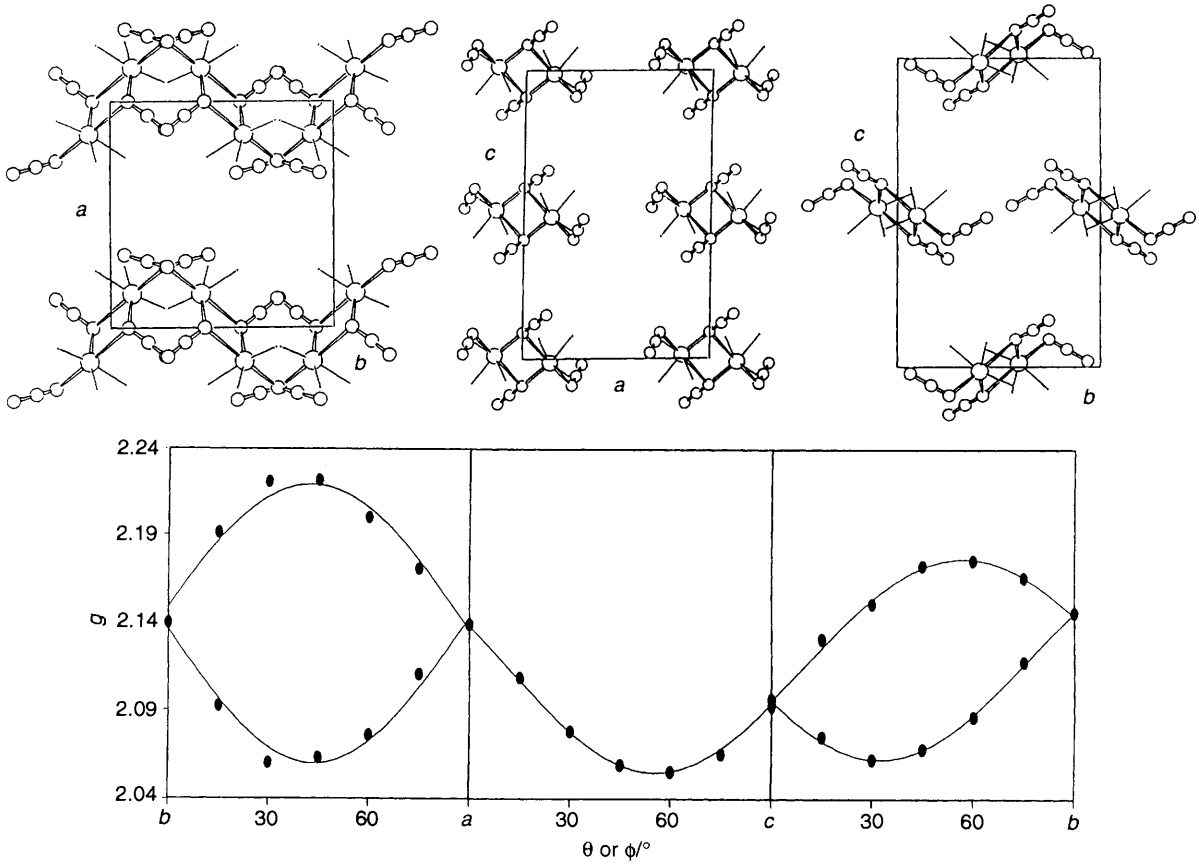

Fig. 5 Angular dependence of the g tensor in the *ab*, *ac* and *bc* planes, together with views of the crystallographic planes, for $[\{Cu_{0.75}Ni_{0.25}(terpy)(N_3)_2\}_2]\cdot 2H_2O$

Of the four metallic sites in the unit cell, only two are magnetically non-equivalent, and are associated with the two crystallographically different dimeric units. This is in complete accord with the single-crystal EPR results. Based on the experimental orientation matrices in Table 6, we can state that the g components follow the geometry of the molecular entities, *i.e.* the orientation matrices of the g tensors are practically the same as those corresponding to the axes of the molecular entities [Cu–N(4^1), N(2)–Cu–N(3) and N(1)–Cu–N(4)]. Thus, g_1 must be associated with g_z and is parallel to the perpendicular to the mean plane corresponding to the equatorial nitrogen atoms [N(1), N(2), N(3), N(4)]. In the same way, g_2 (associated with g_y) and g_3 (associated with g_x) are located in that plane, approximately along the N(2)–Cu–N(3) and N(1)–Cu–N(4) directions, respectively. These values (2.251, 2.064, 2.054) fully agree with those expected for a slightly rhombically distorted CuN_6 chromophore (see crystallographic section). Analysing the two suggested possibilities for compound **2**, the existence of isolated Cu–Cu and Ni–Ni dimers is in full accord with the single-crystal EPR results, the two observed signals corresponding to the copper(II) dimers, with the nickel(II) dimers being EPR silent. In the case of Cu–Ni complexes and Cu–Cu dimers, additional signals due to a $S = \frac{3}{2}$ state, corresponding to the former EPR-active entity, should also appear. Based on these results, the existence of Cu–Ni complexes must be discarded.

Magnetic Properties.—The thermal evolution of the reciprocal magnetic susceptibility and $\chi_m T$ of $[\{Cu_{0.75}Ni_{0.25}(terpy)(N_3)_2\}_2]\cdot 2H_2O$ in the range 4.2–250 K is shown in Fig. 6. Owing to the unusual nature of this compound, magnetic measurements were carried out on polycrystalline samples obtained from large individual crystals (about 8 mg). The existence of a unique phase in the employed powder was corroborated by powder diffraction methods (FULLPROF[22])

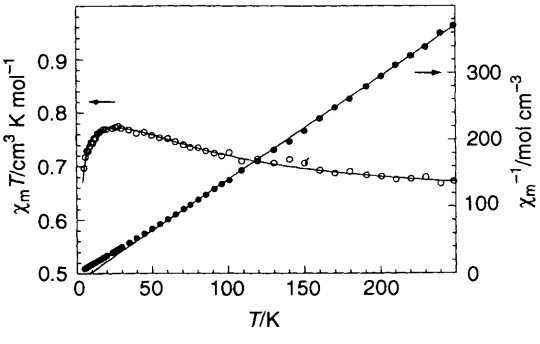

Fig. 6 Thermal variation of the reciprocal susceptibility and $\chi_m T$ for $[\{Cu_{0.75}Ni_{0.25}(terpy)(N_3)_2\}_2]\cdot 2H_2O$

considering the lattice parameters of compound **2**. The high-temperature data ($T > 70$ K) were fitted to a Curie–Weiss law, with $\theta = +8.7$ K and the molar Curie constant 0.65 cm^3 K per mol of metal ions. The positive intercept indicates that the main magnetic interactions are ferromagnetic. The C_m value obtained implies that around 20% of the metal sites are occupied by Ni^{2+} ions, in good agreement with the chemical analysis. The plot of $\chi_m T$ *vs.* T exhibits the same features generally observed for ferromagnetic nickel(II) dimers where the effective magnetic moment increases with decreasing temperature (down to 28 K) and decreases at low temperatures.[2,4] Magnetic coupling between copper(II) ions in dimers with this type of structure appears to be very weak [1,5] and it can be considered that it is not apparent in the susceptibility curve. This is not surprising taking into account that in the copper dimer the exchange pathway lies on a normal to the magnetic orbital.

On the other hand, and considering the EPR spectroscopic

results indicating the absence of mixed Cu–Ni complexes, one can separate the magnetic contributions due to the nickel(II) ions from those due to the Cu^{II}. Therefore, the experimental data can be interpreted with expression (2) where ρ is the proportion

$$\chi = \rho\chi_{Cu} + (1 - \rho)\chi_{Ni} \quad (2)$$

of dimeric $Cu(N_3)_2Cu$ entities, for which the susceptibility is assumed to follow the Curie law: $\chi_{Cu} = Ng_{Cu}^2\beta^2/4kT$. The magnetic susceptibility of the nickel(II) dimers was evaluated by using the analytical expression derived by Ginsberg *et al.*,[23] so lengthy that it is not reproduced here, based upon the spin Hamiltonian (3). The term D represents the usual zero-field

$$H = -2JS_1S_2 - D(S_{1z}^2 + S_{2z}^2) - g\beta H(S_1 + S_2) \quad (3)$$

splitting of the $^3A_2$ ground state of Ni^{II}, a positive value corresponding to the doublet being below the singlet. Least-squares fitting led to the values $J = +20.1$ cm^{-1}, $D = -12.5$ cm^{-1}, $g_{Ni} = 2.26$ and $\rho = 0.76$. The agreement factor, defined as $SE = [\Phi/(n - K)]^{\frac{1}{2}}$ where n is the number of data points (47), K is the number of adjustable parameters (4), and $\Phi = \Sigma(\chi_m T_{obs} - \chi_m T_{calc})^2$ is the sum of squares of the residuals, is equal to 2×10^{-3}. The g_{Cu} value was fixed at 2.123 as determined from the EPR results. The calculated curve is represented by the solid line in Fig. 6, showing excellent agreement with the experimental data.

As expected, the calculated J and D values are very similar to those previously determined for the $[\{Ni(terpy)(N_3)_2\}_2]\cdot 2H_2O$ dimer.[2] In the present case, the introduction of an interdimer exchange term, treated in the molecular field approximation, did not improve the fit. This fact is in good agreement with the relatively low proportion of nickel(II) dimers present in the compound (24%), approximately the same as the value obtained from atomic absorption analysis. It should be noted that small variations in this percentage significantly alter the fit.

Therefore, the observed magnetic behaviour of $[\{Cu_{0.75}Ni_{0.25}(terpy)(N_3)_2\}_2]\cdot 2H_2O$ can be accounted by means of intradimeric ferromagnetic coupling associated with a large nickel(II) single-ion zero-field splitting. The ferromagnetic coupling results in increasing population of the $S = 2$ molecular ground state and thus the effective magnetic moment increases when the temperature is lowered. The effect of the zero-field splitting is a depopulation into a diamagnetic ground state and hence the low-temperature decrease observed in $\chi_m T$.

Conclusion

Two unusual products have been characterised in this study. Complex **1** represents the first co-ordination compound with both halide and pseudohalide ligands. Its synthesis requires very slow donation of azide ligands to the starting chloride compound, which can be achieved by slow addition of an azido complex as donor. The EPR measurements, both on the powder and single crystal, for compound **2** corroborate the existence of Cu–Cu and not mixed Cu–Ni complexes. The single-crystal EPR analysis of this compound, where Ni^{II} is not observed, shows an antiferrodistortive ordering of the two magnetically non-equivalent sites for the copper ions. The magnetic results can be explained by contributions from the two isolated systems, giving rise to a global ferromagnetic behaviour due to the nickel dimer entities. The chemical analysis is in good agreement with the proportion obtained from the fit of the magnetic measurements. From the magnetic data for complex **2** it can be concluded that it consists of isolated Cu–Cu and Ni–Ni units, in *ca.* 75%–25% proportion. The structure of the pure copper(II) compound is monomeric, however the presence of a certain proportion of nickel seems to stabilise the dimeric structure, making the copper adopt the dimeric nickel structure.

Acknowledgements

This work has been financially supported by Grants-in-Aid for Scientific Research from the Ministerio de Educación y Ciencia (DGICYT PB90-0549) and the Universidad del Pais Vasco/Euskal Herriko Unibertsitatea (UPV/EHU 130.310-EB017/92), which we gratefully acknowledge. We thank Professor D. Reinen (Marburg University, Germany) for use of the Varian E15 spectrometer in his laboratory for the single-crystal EPR measurements.

References

1 T. Rojo, R. Cortés, L. Lezama, J. L. Mesa, J. L. Via and M. I. Arriortua, *Inorg. Chim. Acta*, 1989, **165**, 91.
2 M. I. Arriortua, R. Cortés, L. Lezama, T. Rojo, X. Solans and M. Font-Bardia, *Inorg. Chim. Acta*, 1990, **174**, 263.
3 T. Rojo, R. Cortés, M. K. Urtiaga, L. Lezama, G. Villeneuve and M. I. Arriortua, *J. Chem. Soc., Dalton Trans.*, 1991, 1771.
4 R. Cortés, M. K. Urtiaga, L. Lezama, J. I. R. Larramendi, M. I. Arriortua and T. Rojo, *J. Chem. Soc., Dalton Trans.*, 1992, 2723.
5 R. Cortés, M. K. Urtiaga, L. Lezama, J. I. R. Larramendi, M. I. Arriortua and T. Rojo, *J. Chem. Soc., Dalton Trans.*, 1993, 3685.
6 D. M. Duggan and D. N. Hendrickson, *Inorg. Chem.*, 1973, **12**, 2422.
7 D. M. Duggan and D. N. Hendrickson, *Inorg. Chem.*, 1974, **13**, 2929.
8 E. J. Laskowsky, D. M. Duggan and D. N. Hendrickson, *Inorg. Chem.*, 1975, **14**, 2449.
9 A. Escuer, R. Vicente and J. Ribas, *J. Magn. Magn. Mater.*, 1992, **110**, 181.
10 P. Chaudhuri, M. Guttman, D. Ventur, K. Wieghardt, B. Nuber and J. Weiss, *J. Chem. Soc., Chem. Commun.*, 1985, 1618.
11 T. Rojo, M. Vlasse and D. Beltran, *Acta Crystallogr., Sect. C*, 1983, **39**, 194.
12 J. Via, M. I. Arriortua, T. Rojo, J. L. Mesa and A. Garcia, *Bull. Soc. Chim. Belg.*, 1989, **98**, 179.
13 M. C. Burla, G. Carralli, G. Cascarano, G. Giaccovazzo, R. Spagna and D. Vitervo, SIR 88, A Direct Methods Program for the Automatic Solution of Crystal Structures, *J. Appl. Crystallogr.*, 1989, **22**, 389; J. Weller, *J. Appl. Crystallogr.*, 1989, **22**, 19.
14 J. M. Stewart, F. A. Kundell and J. C. Baldwin, X-RAY 72 System, Computer Science Center, University of Maryland, College Parj., MA, 1976.
15 International Tables for X-Ray Crystallography, Kynoch Press, Birmingham, 1974, vol. 4, p. 99.
16 C. K. Johnson, ORTEP, Report ORNL-3794, Oak Ridge National Laboratory, Oak Ridge, TN, 1965.
17 B. J. Hathaway, *Coord. Chem. Rev.*, 1983, **52**, 87; *Comprehensive Coordination Chemistry*, eds. G. Wilkinson, R. D. Gillard and J. A. McCleverty, Pergamon, Oxford, 1985, vol. 5, p. 601.
18 W. Henke, S. Kremer and D. Reinen, *Inorg. Chem.*, 1983, **22**, 2858.
19 E. L. Muetterties and J. L. Guggenberger, *J. Am. Chem. Soc.*, 1974, **96**, 1748.
20 D. L. Kepert, E. S. Kucharski and A. H. White, *J. Chem. Soc., Dalton Trans.*, 1980, 1932.
21 J. Nelson and S. M. Nelson, *J. Chem. Soc. A*, 1969, 1597.
22 J. Rodriguez-Carvajal, FULLPROF, Rietveld Pattern Matching Analysis of Powder Patterns, ILL, Grenoble, 1990.
23 A. P. Ginsberg, R. L. Martin, R. W. Brookes and R. C. Sherwood, *Inorg. Chem.*, 1972, **11**, 2884.

Received 11*th February* 1994; *Paper* 4/00855C